

## B-decay branching fractions, helicities and lifetime measurements in ATLAS

---

**R. Novotný, on behalf of the ATLAS collaboration**

*Department of Physics and Astronomy, University of New Mexico, Albuquerque, NM, USA, 87131*

*E-mail: [radek.novotny@cern.ch](mailto:radek.novotny@cern.ch)*

The ATLAS experiment has an extensive research program focusing on various aspects of heavy flavor decays. Operating LHC experiments at a center-of-mass energy  $\sqrt{s} = 13$  TeV opens new opportunities to measure the properties of the  $B$  hadrons precisely. The first part of this paper focuses on the most recent measurement of the  $B_c^+$  rare decay, which is reconstructed in the  $B_c^+ \rightarrow J/\psi D_s^{(*)+}$  decay channel. The second part of this paper presents an overview of b-hadron measurements performed by the ATLAS experiment involving lifetime parameters.

*21st International Conference on B-Physics at Frontier Machines (Beauty2023)  
3-7 July, 2023  
Clermont-Ferrand, France*



## 1. Study of $B_c^+ \rightarrow J/\psi D_s^{(*)+}$ decays

The pp collisions at the LHC [1] provide rich possibilities for studies of  $B_c$  decays and many properties were already measured in LHC Run1. The first measurement of the  $B_c$  with the ATLAS detector [2] was made in the  $B_c^+ \rightarrow J/\psi \pi^+$  decay channel [3]. The Run1 data also revealed the existence of a new excited state  $B_c(2S)$  that was first observed by the ATLAS experiment [4].

Operating LHC experiments at a center-of-mass energy  $\sqrt{s} = 13$  TeV opens new opportunities to measure the properties of the  $B_c$  meson precisely. Previous studies were limited by the low  $B_c$  production cross-section. The ATLAS experiment focused on the measurement of the  $B_c^+ \rightarrow J/\psi D_s^+$  and  $B_c^+ \rightarrow J/\psi D_s^{*+}$  decays using a data sample with an integrated luminosity of  $139 \text{ fb}^{-1}$  [5]. In this channel,  $B_c$  decays can occur through a weak transition of either heavy quark as well as through a weak annihilation. The study of the  $B_c$  decays in the  $B_c^+ \rightarrow J/\psi D_s^+$  and  $B_c^+ \rightarrow J/\psi D_s^{*+}$  channels, can improve understanding of these production processes.

The  $B_c^+ \rightarrow J/\psi D_s^+$  decay is reconstructed via the cascade fit of its products, where  $J/\psi$  mesons are built from pairs of oppositely charged muon candidates. The  $D_s^+$  meson is reconstructed via the  $D_s^+ \rightarrow \phi \pi^+$  decay. The  $\phi$  candidate is built from two oppositely charged tracks that lie in the invariant mass range of  $\pm 7$  MeV around the world average value. Only three-track combinations successfully fitted to a common vertex are accepted for further analysis as a  $D_s^+$  candidate. The  $D_s^{*+}$  meson decays into a  $D_s^+$  meson and a soft photon or  $\pi^0$  which is not reconstructed in the analysis; however, the mass difference between the  $D_s^+$  and  $D_s^{*+}$  is sufficient for the two decay signals to be resolved as distinct structures in the reconstructed mass of the  $J/\psi D_s^+$  system as shown in Figure 1.

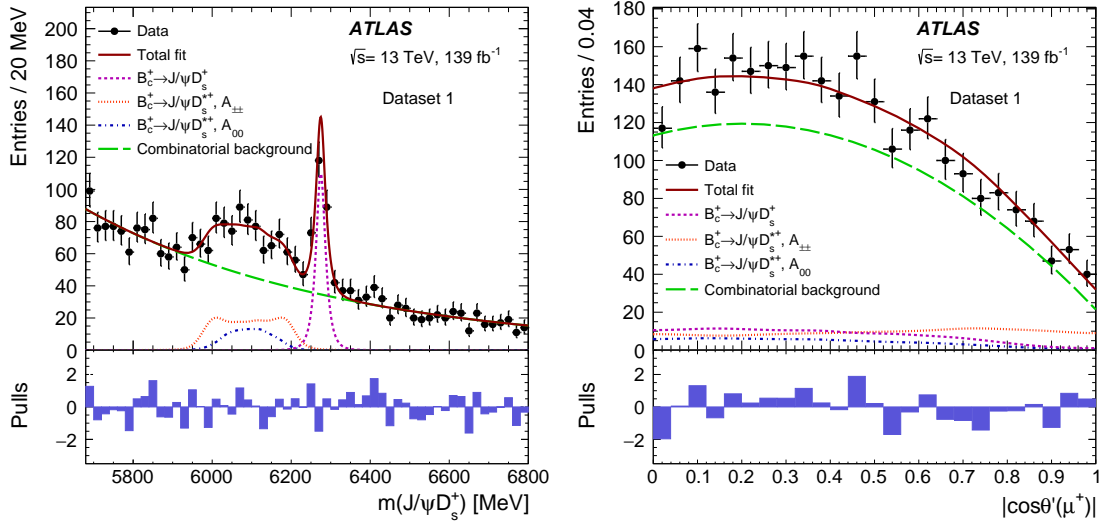


**Figure 1:** Fit projection to  $m(J/\psi D_s^+)$  invariant mass (left) and  $|\cos \theta'(\mu^+)|$  (right) distributions using Dataset 1. Taken from [5].

The information about the helicity in the  $B_c^+ \rightarrow K/\Psi D_s^{*+}$  decay is encoded in the  $J/\Psi D_s^+$  mass spectrum and in the distribution of  $|\cos \theta'(\mu^+)|$ , where  $\theta'(\mu^+)$  is the helicity angle defined in the rest frame of the muon pair as the angle between the  $\mu^+$  and  $D_s^+$  candidate momenta. Since  $B_c^+ \rightarrow J/\psi D_s^{*+}$  is a decay of a pseudoscalar meson into two vector states, the final distributions can

be described in terms of three helicity amplitudes:  $A_{--}$ ,  $A_{++}$  and  $A_{00}$ . However, by studying the Monte Carlo (MC) simulation of the mass  $m(J/\psi D_s^+)$  and  $|\cos \theta'(\mu^+)|$  spectra it was found that the  $A_{++}$  and  $A_{--}$  amplitudes are the same (together called  $A_{\pm\pm}$ ), so the model can be parametrized by the  $A_{\pm\pm}$  and  $A_{00}$  amplitudes and their relative fraction  $f_{\pm\pm}$ . The  $m(J/\psi D_s^+)$  and  $|\cos \theta'(\mu^+)|$  shapes of the two helicity components of the  $B_c^+ \rightarrow J/\psi D_s^{*+}$  signal are described using templates made from the MC simulated events with the adaptive kernel estimation technique. The analysis is performed on two datasets, Dataset 1 contains events collected by di-muon triggers or by three-muon triggers without requirements on the additional Inner Detector (ID) tracks, and Dataset 2 uses events collected only by the dedicated  $B_s^0 \rightarrow \mu^+ \mu^- \phi$  triggers. An extended unbinned maximum likelihood fit to the two-dimensional distribution of  $m(J/\psi D_s^+)$  and  $|\cos \theta'(\mu^+)|$  is performed on both datasets simultaneously, and its results are shown in Table 1. The signal and background probability density functions (PDFs) for the fit are assumed to be uncorrelated for  $m(J/\psi D_s^+)$  and  $|\cos \theta'(\mu^+)|$ . The projection of the fit onto the  $J/\psi D_s^+$  invariant mass and  $|\cos \theta'(\mu^+)|$  distributions using Dataset 1 is shown in Figure 1. Since the datasets are fitted simultaneously, two yields,  $N_{B_c^+ \rightarrow J/\psi D_s^+}^{DS1}$  and  $N_{B_c^+ \rightarrow J/\psi D_s^+}^{DS2}$ , are published.

Par.	$m_{B_c^+}$ [MeV]	$\sigma_{B_c^+}$ [MeV]	$r_{D_s^{*+}/D_s^+}$	$f_{\pm\pm}$	$N_{B_c^+ \rightarrow J/\psi D_s^+}^{DS1}$	$N_{B_c^+ \rightarrow J/\psi D_s^+}^{DS2}$
Val.	$6274.8 \pm 1.4$	$11.5 \pm 1.5$	$1.76 \pm 0.22$	$0.70 \pm 0.10$	$193 \pm 20$	$49 \pm 10$
Par.	$N_{B_c^+ \rightarrow J/\psi D_s^{*+}}^{DS1}$	$N_{B_c^+ \rightarrow J/\psi D_s^{*+}}^{DS1\&2}$	$N_{B_c^+ \rightarrow J/\psi D_s^{*+}}^{DS1\&2}$			
Val.	$338 \pm 32$	$241 \pm 28$	$424 \pm 46$			

**Table 1:** Parameters of the  $B_c^+ \rightarrow J/\psi D_s^+$  and  $B_c^+ \rightarrow J/\psi D_s^{*+}$  signals obtained with the unbinned extended maximum likelihood fit to the data. Only the statistical uncertainties are included. No acceptance or efficiency corrections are applied to the signal yields. Taken from [5].

The reference channel  $B_c^+ \rightarrow J/\psi \pi^+$  is used for both decays. Partially reconstructed  $B_c^+$  decays (PRDs),  $B_c^+ \rightarrow J/\psi X$ , as well as the peaking background from  $B_c^+ \rightarrow J/\psi K^+$ , are modeled by the MC simulation shapes. The yield is extracted with an extended unbinned maximum-likelihood fit. The ratios of the branching fractions for the  $J/\psi D_s^{(*)+}$  and  $B_c^+ \rightarrow J/\psi \pi^+$  decays are given by

$$R_{D_s^{(*)+}/\pi^+} = \frac{\mathcal{B}(B_c^+ \rightarrow J/\psi D_s^{(*)+})}{\mathcal{B}(B_c^+ \rightarrow J/\psi \pi^+)},$$

and the ratio of the branching fractions to  $J/\psi D_s^{*+}$  and  $J/\psi D_s^+$  is given by

$$R_{D_s^{*+}/D_s^+} = \frac{\mathcal{B}(B_c^+ \rightarrow J/\psi D_s^{*+})}{\mathcal{B}(B_c^+ \rightarrow J/\psi D_s^+)}.$$

The measured ratios are found to be  $R_{D_s^+/\pi^+} = 2.76 \pm 0.33(\text{stat.}) \pm 0.29(\text{syst.}) \pm 0.16(\text{ext.})$ ;  $R_{D_s^{*+}/\pi^+} = 5.33 \pm 0.61(\text{stat.}) \pm 0.67(\text{syst.}) \pm 0.32(\text{ext.})$ ; and  $R_{D_s^{*+}/D_s^+} = 1.93 \pm 0.24(\text{stat.}) \pm 0.09(\text{syst.})$ , where the first uncertainty is statistical, the second is systematic, and the third corresponds to the external uncertainty in the branching fraction of the normalization channel. In addition to the ratios of the branching fractions, the transverse polarization fraction  $\Gamma_{\pm\pm}/\Gamma$  in the  $B_c^{*+} \rightarrow J/\psi D_s^{*+}$  decays, defined as follows,

$$\Gamma_{\pm\pm}/\Gamma = f_{\pm\pm} \frac{\epsilon_{B_c^+ \rightarrow J/\psi D_s^{*+}}^{DS1\&2}}{\epsilon_{B_c^+ \rightarrow J/\psi D_s^{*+}, A_{\pm\pm}}},$$

is measured to be  $\Gamma_{\pm\pm}/\Gamma = 0.70 \pm 0.10(\text{stat.}) \pm 0.04(\text{syst.})$ . All results are compared to the previous measurements by ATLAS [6] and LHCb [7] as well as to the theory predictions as shown in Figure 2. The QCD relativistic potential model [8] was found to be in the best agreement with the obtained results.

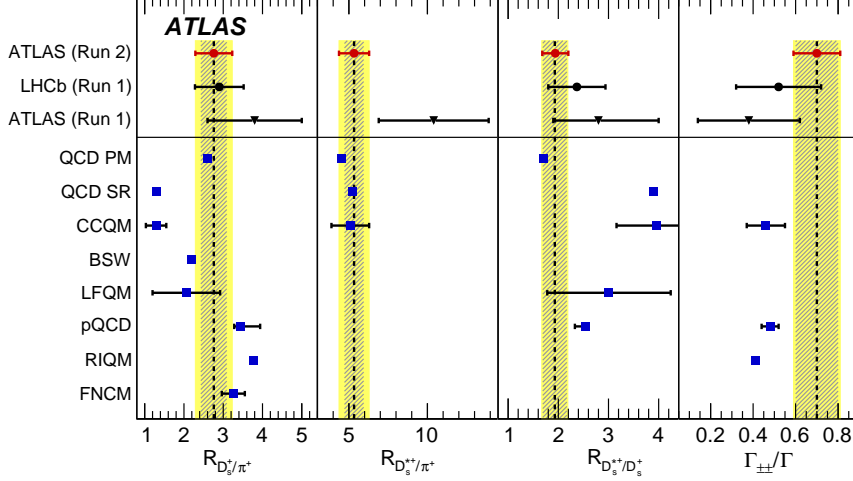


**Figure 2:** Comparison of the results of this measurement with those of ATLAS Run1 and LHCb, and with the theoretical predictions based on a QCD relativistic potential model (QCD PM), QCD sum rules (QCD SR), the covariant confined quark model (CCQM), the Bauer&Stech&Wirbel relativistic quark model (BSW), the light-front quark model (LFQM), perturbative QCD (pQCD), the relativistic independent quark model (RIQM), and calculations in the QCD factorization approach (FNMC). Hatched areas show the statistical uncertainties of this measurement, and yellow bands correspond to the total uncertainties. Quadrature sums of all experimental uncertainties are quoted for the ATLAS Run1 and LHCb results. The uncertainties on the theoretical predictions are shown only if they are explicitly quoted in the corresponding papers. Taken from [5].

## 2. Overview of lifetime measurements performed by ATLAS

The ATLAS experiment has a rich history of B-meson lifetime measurements in various channels. Some of the channels are rare and hardly accessible by other experiments, so the obtained results are very valuable. This section will summarize the most recent measurements and those that pushed the limits in the field.

### 2.1 $\Lambda_b^0$ lifetime measurement

The most direct lifetime measurement was performed for the  $\Lambda_b^0$  baryon decay where the  $\Lambda_b^0$  is reconstructed in the decay chain  $\Lambda_b^0 \rightarrow J/\psi \Lambda^0$  [9]. The decay  $\Lambda_b^0 \rightarrow J/\psi \Lambda^0$  has a cascade topology, where the  $J/\psi$  decays instantly at the same point as the  $\Lambda_b^0$  production (the secondary vertex), while the  $\Lambda^0$  lives long enough to form a displaced tertiary vertex. There are four final state particles: two muons from the  $J/\psi$ , and a proton and a pion from the  $\Lambda^0$  decay.

The analysis uses on data collected in LHC Run1 using single-muon, dimuon, and  $J/\psi$  triggers. An unbinned maximum likelihood fit is used to determine the  $\Lambda_b^0$  mass and lifetime

parameters. The fit projections are shown in Figure 3. The measured invariant mass of the  $\Lambda_b$  is  $m_{\Lambda_b} = 5619.7 \pm 0.7$  MeV, and the lifetime  $\tau_{\Lambda_b} = 1.449 \pm 0.036$  ps.

The  $B_d^0 \rightarrow J/\psi K_S^0(\pi^+\pi^-)$  channel has the same decay topology as  $\Lambda_b^0 \rightarrow J/\psi \Lambda^0(p\pi^-)$  and can be used to cross-check the  $\Lambda_b^0$  results and to determine the ratio of the  $\Lambda_b^0$  and  $B_d^0$  lifetimes. The  $B_d^0$  channel is subjected to exactly the same kinematic cuts as the  $\Lambda_b^0$ . Using the maximum likelihood fit, the  $B_d^0$  lifetime and mass are measured to be  $\tau_{B_d} = 1.509 \pm 0.012(\text{stat}) \pm 0.018(\text{syst})$  ps and  $m_{B_d} = 5279.6 \pm 0.2(\text{stat}) \pm 1.0(\text{syst})$  MeV. This allows us to measure the ratio of the  $\Lambda^0$  and  $B_d^0$  lifetimes as:

$$R = \tau_{\Lambda_b} / \tau_{B_d} = 0.960 \pm 0.025(\text{stat}) \pm 0.016(\text{syst}).$$

The results are the most precise ATLAS measurement in this channel.

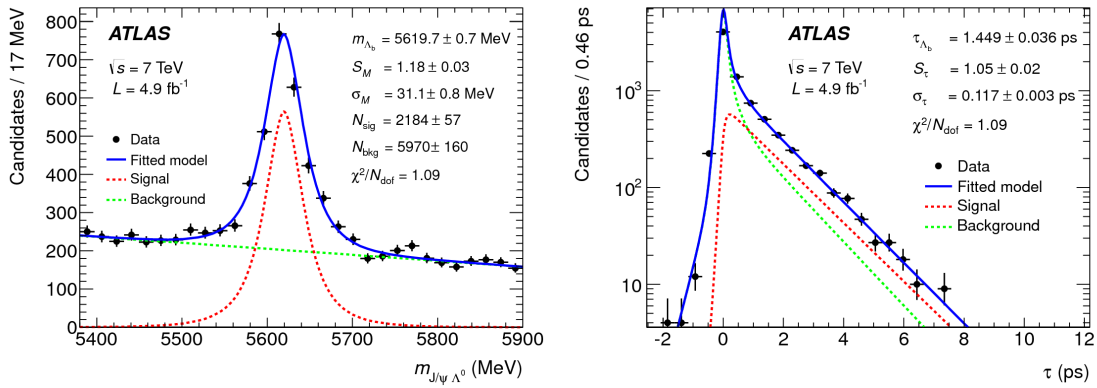


**Figure 3:** Projections of the fitted PDF onto the mass  $m(J/\Psi\Lambda^0)$  and lifetime  $\tau$  of the  $\Lambda_b^0$  candidates. The errors of the listed fit result values are statistical only. The  $\chi^2/N_{\text{dof}}$  value is calculated from the data set binned in mass and decay time with the number of degrees of freedom,  $N_{\text{dof}} = 61$ . Taken from [9].

## 2.2 Measurement of the CP-violating phase in $B_s \rightarrow J/\psi\phi$

The most recent measurement that yields lifetime parameters is the measurement of CP-violation in  $B_s \rightarrow J/\psi\phi$  events [10]. The main goal of this analysis is the measurement of the CP-violating phase,  $\phi_s$ , which is potentially sensitive to New Physics (NP), however; the lifetime parameters of the  $B_s \rightarrow J/\psi\phi$  are also measured and provide important information for understanding this system. The lifetime parameters in  $B_s^0$  mixing are  $\Delta\Gamma_s = \Gamma_s^L - \Gamma_s^H$ , where  $\Gamma_s^L$  and  $\Gamma_s^H$  are the decay widths of the different mass eigenstates, and  $\Gamma_s = (\Gamma_s^L + \Gamma_s^H)/2$ , their average. This analysis also involves angular descriptions of the signal events together with the non-resonant S-wave that are described by the following set of amplitudes ( $A$ ) and strong phases ( $\delta$ ):  $|A_0(0)|^2$ ,  $|A_{||}(0)|^2$ ,  $|A_S(0)|^2$ ,  $\delta_{||}$ ,  $\delta_{\perp}$  and  $\delta_S$ .

The analysis uses a partial Run2 data sample with  $80.5 \text{ fb}^{-1}$  of integrated luminosity. To extract parameters describing the  $B_s \rightarrow J/\psi\phi$  process and the S-wave parameters, an unbinned maximum likelihood fit is performed. The Run2 results show two well-separated local maxima of the likelihood function for the strong-phases  $\delta_{\perp}$  and  $\delta_{||}$ . Their difference in likelihood values is minimal and the impact on other parameters is negligible. The measured values are  $\phi_s = -0.081 \pm 0.041(\text{stat.}) \pm 0.022(\text{syst.})$  rad,  $\Delta\Gamma_s = 0.0607 \pm 0.0047(\text{stat.}) \pm 0.0043(\text{syst.}) \text{ ps}^{-1}$  and

$\Gamma_s = 0.6687 \pm 0.0015(\text{stat.}) \pm 0.0022(\text{syst.}) \text{ ps}^{-1}$ , where the first uncertainty is statistical and the second is systematic. The Run2 results are combined with those from the analysis in Run1 [11], achieving the following results:  $\phi_s = -0.087 \pm 0.036(\text{stat.}) \pm 0.019(\text{syst.}) \text{ rad}$ ,  $\Delta\Gamma_s = 0.0641 \pm 0.0043(\text{stat.}) \pm 0.0024(\text{syst.}) \text{ ps}^{-1}$  and  $\Gamma_s = 0.6697 \pm 0.0014(\text{stat.}) \pm 0.0015(\text{syst.}) \text{ ps}^{-1}$ .

These results are consistent with the SM prediction [12] and other LHC experiments, with only small tensions. The comparison can be seen in the two-dimensional contours in the  $\phi_s - \Delta\Gamma_s$  and  $\Gamma_s - \Delta\Gamma_s$  planes in Figure 4.

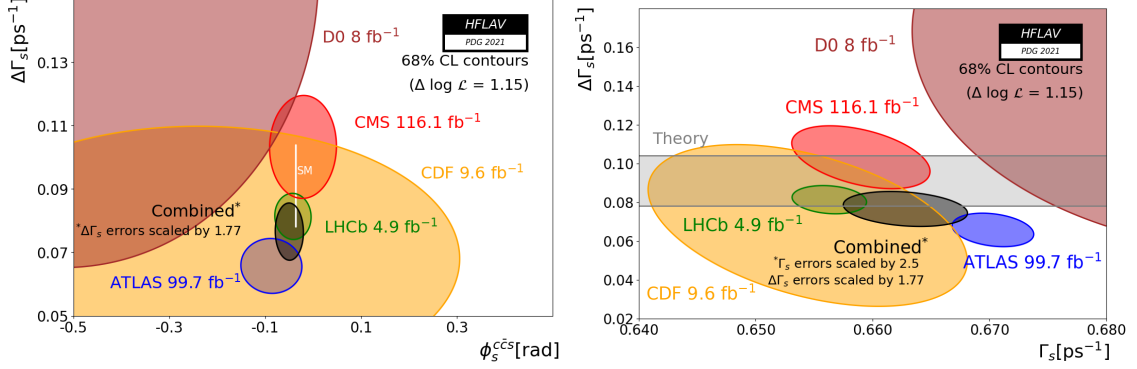


**Figure 4:** Contours of 68% confidence level in the  $\phi_s - \Delta\Gamma_s$  plane (left) and  $\Gamma_s - \Delta\Gamma_s$  plane (right). The plots include results from ATLAS (blue), CMS (red), LHCb (green), CDF (orange) and D0 (brown). The combination of all results, performed by the HFLAV group [13], is shown as a black contour. The Standard Model prediction is shown as a very thin black rectangle. In all contours, the statistical and systematic uncertainties are combined in quadrature. Taken from [13].

### 2.3 $B^0 - \bar{B}^0$ decay width difference

The last measurement presented here is the measurement of the relative width difference  $\Delta\Gamma_d/\Gamma_d$  of the  $B^0 - \bar{B}^0$  system using data collected by the ATLAS experiment at the LHC in pp collisions at  $\sqrt{s} = 7 \text{ TeV}$  and  $\sqrt{s} = 8 \text{ TeV}$  and corresponding to an integrated luminosity of  $25.2 \text{ fb}^{-1}$  [14]. The relative value of  $\Delta\Gamma_d/\Gamma_d$  is predicted in the Standard Model (SM) [15]:  $\Delta\Gamma_d/\Gamma_d(\text{SM}) = (0.42 \pm 0.08) \times 10^{-2}$ . The measurement is based on the fit of the production ratio between  $B^0 \rightarrow J/\psi K_S$  and  $B^0 \rightarrow J/\psi K^{*0}$  decays which depend upon the proper decay length  $L_{\text{prop}}^B$  after correction for detector effects. The proper decay length,  $L_{\text{prop}}^B$ , is defined as  $L_{\text{prop}}^B = \frac{L_{xy}}{p_{TB}} m_B$ , where  $L_{xy}$  is the displacement in transverse plane of the  $B^0$  meson decay vertex relative to the primary vertex,  $p_{TB}$  is the reconstructed transverse momentum and  $m_B$  is the mass of  $B^0$  meson. The relative width difference  $\Delta\Gamma_d/\Gamma_d$  is obtained from a  $\chi^2$  minimization of the binned distributions in the following way:

$$\chi^2[\Delta\Gamma_d/\Gamma_d] = \sum_i \frac{(R_{i,\text{cor}} - R_{i,\text{exp}}[\Delta\Gamma_d/\Gamma_d])^2}{\sigma_i^2},$$

where  $R_{i,\text{cor}}$  corresponds to the corrected production ratio,  $R_{i,\text{exp}}[\Delta\Gamma_d/\Gamma_d]$  is the expected ratio of the decay rates and the  $\sigma_i$  are the statistical uncertainties on  $R_{i,\text{cor}}$ . The fit is performed separately for the 2011 and 2012 samples because the systematic uncertainties for the two data samples are

different. The results of the fits are shown in Figure 5. The combined result for the data collected by the ATLAS experiment in Run1 is  $\Delta\Gamma_d/\Gamma_d = (-0.1 \pm 1.1(\text{stat.}) \pm 0.9(\text{syst.})) \times 10^{-2}$ . It agrees well with the SM prediction and is consistent with other measurements of this quantity.

The analysis also measures the production asymmetry that is defined as follows:

$$A_P = \frac{\sigma(B_q^0) - \sigma(\bar{B}_q^0)}{\sigma(B_q^0) + \sigma(\bar{B}_q^0)},$$

where the  $\sigma$  denotes the production cross-section of the corresponding particle. It can be measured from the time-dependent charge asymmetry of the flavor-specific decay. CP violation in mixing is predicted to be small in the SM and so it is omitted from the asymmetry expression. The production asymmetry of  $B^0$  mesons with  $p_T(B^0) > 10 \text{ GeV}$  and  $|\eta(B^0)| < 2.5$  is found to be

$$A_P(B^0) = (0.25 \pm 0.48 \pm 0.05) \times 10^{-2}.$$

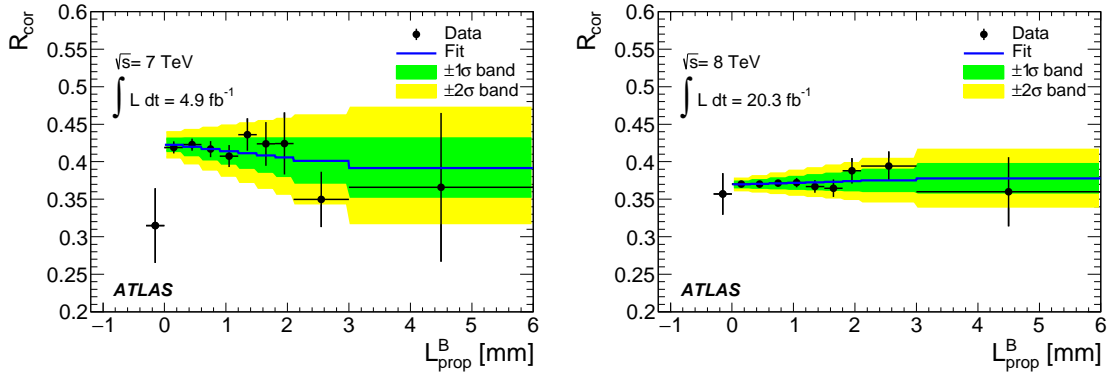


**Figure 5:** Efficiency-corrected ratio of the observed decay length distributions,  $R_{\text{cor}}(L_{\text{prop}}^B)$  for the (a)  $\sqrt{s} = 7 \text{ TeV}$  and (b)  $\sqrt{s} = 8 \text{ TeV}$  data sets. The normalization of the two data sets is arbitrary. The full line shows the fit of  $R_{\text{cor}}(L_{\text{prop}}^B)$  to  $R_{\text{exp}}$ . The error bands correspond to uncertainties in  $\Delta\Gamma_d/\Gamma_d$  determined by the fit. Taken from [14].

### 3. Summary

ATLAS has an extensive research program focusing on various aspects of heavy flavor decays. ATLAS has conducted precise measurements of CP-violation and lifetime parameters as well as studies of rare decays such as  $B_c^+ \rightarrow J/\psi D_s^{(*)+}$ . It provides valuable results for comparison to theoretical predictions and also helps to validate various models.

### Acknowledgments

I acknowledge support from the National Science Foundation grant number 1906674.

## References

- [1] L. Evans and P. Bryant, “LHC Machine,” JINST **3** (2008), S08001
- [2] G. Aad *et al.* [ATLAS], “The ATLAS Experiment at the CERN Large Hadron Collider,” JINST **3** (2008), S08003
- [3] G. Aad *et al.* [ATLAS], “Observation of the  $B_c^\pm$  meson in the decay  $B_c^\pm \rightarrow J/\psi(\mu^+\mu^-)\pi^\pm$  with the ATLAS detector at the LHC,” ATLAS-CONF-2012-028.
- [4] G. Aad *et al.* [ATLAS], “Observation of an Excited  $B_c^\pm$  Meson State with the ATLAS Detector,” Phys. Rev. Lett. **113** (2014) no.21, 212004 [arXiv:1407.1032 [hep-ex]].
- [5] G. Aad *et al.* [ATLAS], “Study of  $B_c^+ \rightarrow J/\psi D_s^+$  and  $B_c^+ \rightarrow J/\psi D_s^{*+}$  decays in  $pp$  collisions at  $\sqrt{s} = 13$  TeV with the ATLAS detector,” JHEP **08** (2022), 087 [arXiv:2203.01808 [hep-ex]].
- [6] G. Aad *et al.* [ATLAS], “Study of the  $B_c^+ \rightarrow J/\psi D_s^+$  and  $B_c^+ \rightarrow J/\psi D_s^{*+}$  decays with the ATLAS detector,” Eur. Phys. J. C **76** (2016) no.1, 4 doi:10.1140/epjc/s10052-015-3743-8 [arXiv:1507.07099 [hep-ex]].
- [7] R. Aaij *et al.* [LHCb], “Observation of  $B_c^+ \rightarrow J/\psi D_s^+$  and  $B_c^+ \rightarrow J/\psi D_s^{*+}$  decays,” Phys. Rev. D **87** (2013) no.11, 112012 [arXiv:1304.4530 [hep-ex]].
- [8] P. Colangelo and F. De Fazio, “Using heavy quark spin symmetry in semileptonic  $B_c$  decays,” Phys. Rev. D **61** (2000), 034012 [arXiv:hep-ph/9909423 [hep-ph]].
- [9] G. Aad *et al.* [ATLAS], “Measurement of the  $\Lambda_b^0$  lifetime and mass in the ATLAS experiment,” Phys. Rev. D **87** (2013) no.3, 032002 [arXiv:1207.2284 [hep-ex]].
- [10] G. Aad *et al.* [ATLAS], “Measurement of the  $CP$ -violating phase  $\phi_s$  in  $B_s^0 \rightarrow J/\psi\phi$  decays in ATLAS at 13 TeV,” Eur. Phys. J. C **81** (2021) no.4, 342 [arXiv:2001.07115 [hep-ex]].
- [11] G. Aad *et al.* [ATLAS], “Measurement of the  $CP$ -violating phase  $\phi_s$  and the  $B_s^0$  meson decay width difference with  $B_s^0 \rightarrow J/\psi\phi$  decays in ATLAS,” JHEP **08** (2016), 147 [arXiv:1601.03297 [hep-ex]].
- [12] J. Charles, O. Deschamps, S. Descotes-Genon, R. Itoh, H. Lacker, A. Menzel, S. Monteil, V. Niess, J. Ocariz and J. Orloff, *et al.* “Predictions of selected flavour observables within the Standard Model,” Phys. Rev. D **84** (2011), 033005 [arXiv:1106.4041 [hep-ph]].
- [13] Amhis, Y. and others “Averages of  $b$ -hadron,  $c$ -hadron, and  $\tau$ -lepton properties as of 2021” Phys. Rev. D **107** (2023), 052008 [arXiv:2206.07501 [hep-ex]].
- [14] M. Aaboud *et al.* [ATLAS], “Measurement of the relative width difference of the  $B^0$ - $\bar{B}^0$  system with the ATLAS detector,” JHEP **06** (2016), 081 [arXiv:1605.07485 [hep-ex]].
- [15] A. Lenz and U. Nierste, “Numerical Updates of Lifetimes and Mixing Parameters of  $B$  Mesons,” [arXiv:1102.4274 [hep-ph]].